JOURNAL OF MODERN OPTICS, 15 FEBRUARY 2004
VOL. 51, NO. 3, 313–332

Taylor & Francis
Taylor & Francis Group

A model of the angular distribution of light scattered by multilayered media

A. DA SILVA†, C. ANDRAUD†, J. LAFAIT†*, T. ROBIN‡ and R. G. BARRERA¶

†Laboratoire d'Optique des Solides de l'Université Pierre et Marie Curie Paris 6, case 80, 4 place Jussieu 75252 Paris Cedex 05 – France
‡Eurêka technologies, 12 rue Bertie Albrecht 92220 Bagneux – France
¶Instituto de Física, Universidad Nacional Autónoma de México, 01000 Mexico D. F., Mexico

(*Received 7 January 2003; final version 24 June 2003*)

Abstract. A model for calculating the spatial distribution of light flux scattered from multilayered inhomogeneous media, with index of refraction mismatches between layers, is described. By separating volume and surface properties, a compact matrix formulation is constructed for the solution of this problem, based on the application of the Discrete Ordinate Method to solve the Radiative Transfer Equation. Results are compared with those obtained with other techniques in order to evaluate the accuracy and efficiency of the proposed method. An optimization of the numerical procedure has been achieved, allowing application of the method to systems with a large number of slabs.

1. Introduction

Knowledge of the optical properties of inhomogeneous media that scatter and absorb light is often required in the solution of many problems in diverse areas of science and technology. A quite useful procedure for the calculation of these properties is based on the solution of the Radiative Transfer Equation (RTE), which was advanced during the 1960s within the context of astrophysical problems [1]. Since then, several numerical procedures to solve this equation have been developed, and currently they are successfully applied in a wide range of systems of interest in different disciplines [2–7].

The RTE is an integro-differential equation commonly solved using the Discrete Ordinate Method (DOM). The origin of this method dates back to the 'Two Flux' approximation of the early 1900s [8–10], and since then methods based on this approximation have been developed and widely applied [11–16]. Because of its conceptual simplicity, the RTE has become one of the most popular techniques in the heat transfer, atmospheric physics, and coatings communities, for solving problems of radiative transfer involving multiple scattering. This technique has been generally applied to the treatment of monolayered scattering media, although they have also been extended to multilayered slabs with no mismatch in the index of refraction between layers [17, 18]. This means that the different layers of scatterers are all embedded in a surrounding medium with the same index

* Corresponding author: lafait@ccr.jussieu.fr

Journal of Modern Optics ISSN 0950–0340 print/ISSN 1362–3044 online © 2004 Taylor & Francis Ltd
http://www.tandf.co.uk/journals
DOI: 10.1080/0950034032000124322

of refraction. Liou *et al.* [19] also suggested a semi-analytical method to treat a two-layered slab in which the embedding matrices of each slab have different indices of refraction, but this approach is restricted to the case of isotropic angular distribution of the scattered light in both layers.

In this paper, we examine radiative transfer through stratified films of scattering media with plane interfaces. The embedding material of each medium has a different index of refraction, and the reflectance and transmittance at each interface are described by Fresnel equations. We construct a compact matrix procedure capable of dealing with the scattering properties of a system of multilayered slabs composed of different scattering layers with index of refraction mismatch at each interface. The structure of this matrix treatment is analogous to non-scattering multilayer calculations [20], in so far as one relates the outgoing flux directly with the incident one.

The second section of the paper is devoted to the description of the DOM, and in the third section we introduce the boundary conditions and explain also how one can deal with the overflow problems often mentioned when solving RTE. In the fourth section we derive expressions for the transfer matrix $\mathbf{Q}$, which accounts in the stratified system for the presence of both the scattering media (absorption and scattering) and the interfaces (reflectance and transmittance). In the fifth section, we first make a comparison of the predictions of our model with predictions obtained using a Monte Carlo method [21] and a 4-flux model [22], as applied to two configurations that illustrate the Rayleigh- and Mie-scattering regimes. We then give one example of a two-layered slab calculation, and finally, one example of a calculation on a system composed of five layers. The last section is devoted to conclusions.

2. *N*-flux model

The RTE is a macroscopic description of radiation transfer and stems from a balance of the energy flux on a volume element located within the scattering system. RTE describes the spatial evolution of the flux intensity $I(\mathbf{r}, \mathbf{u}, t)$, at a point $\mathbf{r}$, in a direction $\mathbf{u}$, at time t. The properties of the scattering medium are then totally specified by three parameters: the absorption and scattering coefficients, defined per unit volume, and the phase function.

Within the framework of this paper, the properties of the medium are considered in the steady-state regime, that is, the boundary conditions do not depend upon time. But let us first describe the geometry of the system. The scattering medium is bounded by parallel planes which extend over a region whose size is very large compared to its thickness, thus the boundary conditions and the formulas here derived do not depend upon the position along the planes. These two restrictions allow the effective removal of two dimensions, leaving only the linear coordinate perpendicular to the boundary planes (z), as a position parameter, and the polar and azimuthal angles (θ, ϕ). Furthermore, the medium is assumed to be passive, although this restriction can be easily removed if emission or fluorescence are introduced into the equations as linear effects. However, the most important limitation in the following equations is the neglect of polarization. It has been shown that this approximation causes the largest errors when the optical thickness of the scattering medium is small [23]. Schulz *et al.* [24] propose a solution to account for polarization in multilayered slabs, in the very restricted case

where there is no refractive index mismatch in the system. Kim *et al*. [25] suggest another treatment based on decomposition of the specific intensity into Chebyshev polynomials. Our matrix technique can also be extended to account for light polarization by introducing, as in the references mentioned above, Mueller matrices to express the emerging flux as Stokes vectors.

Figure 1 shows the coordinate system used to set up the RTE: the space is divided into N conical solid angles corresponding to N channels (N must be even). The forward direction corresponds to channel numbers i belonging to [1, $N/2$], and the backward direction to i belonging to $[N/2+1, N]$. Light traveling between θ_{i-1} and θ_i is defined as belonging to channel i.

The specific intensity I, and the flux F are related by $F = I\cos\theta \mathrm{d}\omega$, where θ is the angle between the detection direction **u** and the normal to the boundary planes and $\mathrm{d}\omega$ is the unit solid angle. However, the flux in a channel with a large solid angle has to be calculated from the specific intensity by an integration of the form

$$F = \int I \cos\theta \frac{\mathrm{d}\omega}{2\pi},$$

(see figure 2), and the integration extends over all angles in the channel. Here we shall only work with flux.

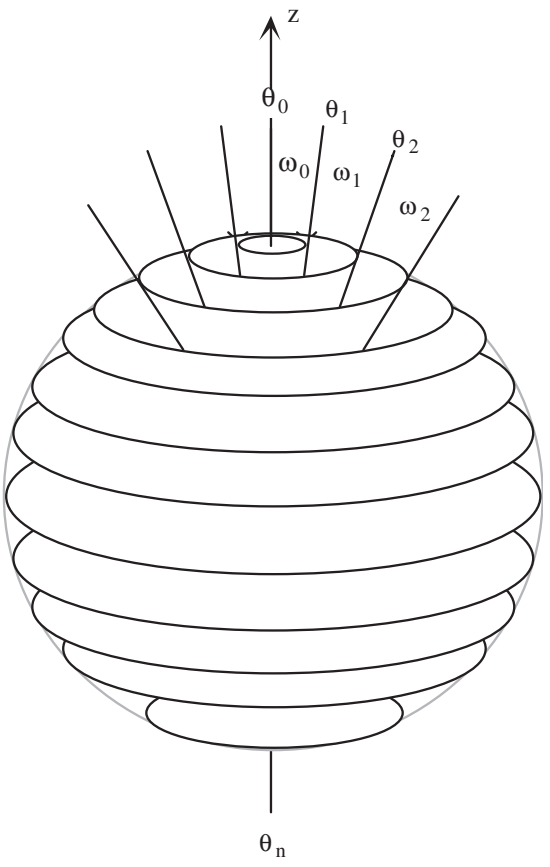

Figure 1. Space discretization for N-flux model.

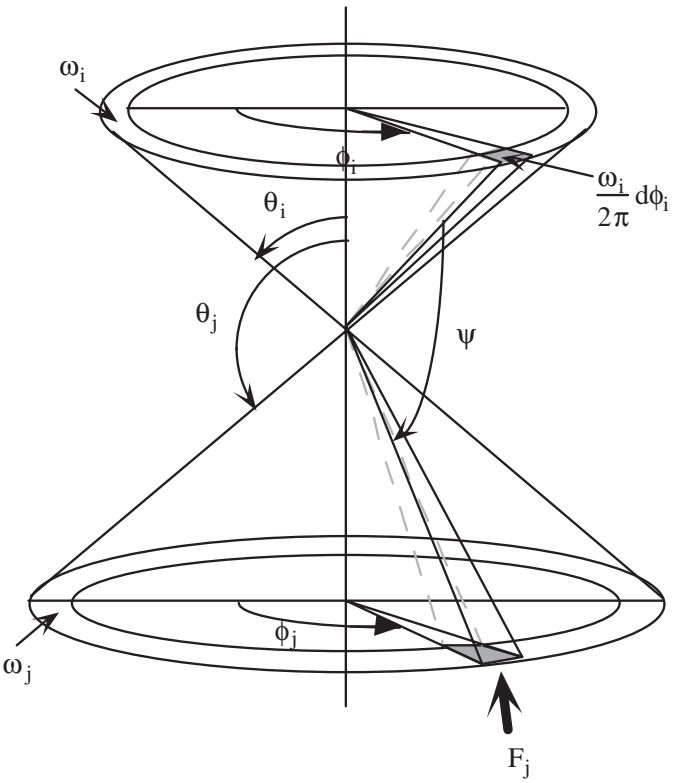

Figure 2. Definition of a channel.

2.1. *Discrete radiative transfer equation and general solution*

Taking into account the previous assumptions, we propose a new formulation for the calculation of the reflected and transmitted flux through a multislab system composed of non-absorbing materials containing spherical absorbing particles. This treatment is inspired by Mudgett's paper [14] in relation to the space discretization and to the scattered-flux formulation.

The evolution of a light flux F in a scattering medium is governed by the RTE, which can be expressed for the steady state, as follows:

$$\underbrace{\frac{\partial F(z,\mathbf{u})}{\partial z}}_{\substack{\text{flux variation}\\ \text{in element d}z}} = -\underbrace{\frac{k_{\text{ext}}}{\cos\theta}F(z,\mathbf{u})}_{\substack{\text{loss by scattering}\\ \text{and absorption}\\ \text{in direction } \mathbf{u}}} + \underbrace{k_{\text{sca}}\int_{4\pi}\frac{F(z,\mathbf{u}')}{\cos\theta'}\frac{p(\mathbf{u}.\mathbf{u}')}{4\pi}\,\mathrm{d}\omega'}_{\substack{\text{gain by scattering}\\ \text{from all directions } \mathbf{u}'\\ \text{towards direction } \mathbf{u}}} \tag{1}$$

where $\mathbf{u}$ is the detection direction, and k_{ext} and k_{sca} the extinction and the scattering coefficients, respectively, defined per unit length. $F(z,\mathbf{u})$ denotes the total flux at the position z in the medium, and scattered in direction $\mathbf{u}$. The phase function $p(\mathbf{u}.\mathbf{u}')/4\pi$ represents the probability that radiation, incident in direction $\mathbf{u}'$, is scattered in direction $\mathbf{u}$. If we now assume that the volume fraction of particles is small, so one can regard the scattering process as a series of independent events (independent scattering), the phase function in equation (1) will correspond to the phase function of an independent scatterer. In the case of

spherical scatterers and if light polarization is neglected, the phase function will depend only on the scattering angle.

Let us now assume that the system is isotropic and it is illuminated by a collimated flux F_0 incident at an angle θ_0 with respect to the normal to the boundary planes. The expression for the collimated flux at z is then $F_{\text{coll}}(z) = F_0 \exp(-k_{\text{ext}} z/\cos\theta_0)$. But in the following treatment we will consider, for simplicity, only normal illumination. If this were not the case, it can be shown [1] that one can decouple the ϕ and θ contributions by expressing the flux as a Fourier series over the azimuthal angle ϕ. One then obtains a set of decoupled equations with the same form as equation (1).

The numerical procedure to solve equation (1) starts by the numerical evaluation of the integral using the DOM [1], which assumes a space discretization in $\cos\theta$ (Gauss discretization). The number of channels that have to be taken into account to evaluate this integral with good accuracy depends on the anisotropy of the phase function. This will be discussed in more detail in section 5. For a system discretized into N channels, the differential equations describing the radiative transfer problem can be written as:

$$\begin{cases} \dfrac{\mathrm{d}F_i}{\mathrm{d}z} = \displaystyle\sum_{j=1}^{N} \mathrm{s}_{ij} F_j, & i \le N/2 \\ -\dfrac{\mathrm{d}F_i}{\mathrm{d}z} = \displaystyle\sum_{j=1}^{N} \mathrm{s}_{ij} F_j, & i > N/2 \end{cases} \tag{2}$$

where F_i is the monochromatic flux in channel i, s_{ij} the coefficient describing scattering from channel j into channel i, and z the perpendicular distance to the boundary planes. For $j = i$ the coefficient s_{jj} corresponds to the total scattering from channel j into all other channels plus the attenuation due to absorption in channel j, namely the total extinction. The coefficients s_{ij} form a matrix with dimension $N \times N$, and equation (2) can then be written in a more compact form as,

$$\frac{\mathrm{d}\mathbf{F}}{\mathrm{d}z} = \mathbf{SF}; \qquad S_{ij} = \mathrm{s}_{ij} \text{ if } i \le N/2; \qquad S_{ij} = -\mathrm{s}_{ij} \text{ if } i > N/2, \tag{3}$$

where $\mathbf{S}$ is the matrix notation for S_{ij} in which the terms on the diagonal represent loss by scattering and absorption while terms outside the diagonal represent gain by scattering. Here $\mathbf{F}$ is a vector $[F_1, F_2, \ldots, F_N]^{\mathrm{t}}$, where each component represents the magnitude of the flux in a given channel and the superscript t means transpose. By using the unit matrix $\mathbf{I}$, equation (3) can be rewritten as

$$\frac{\mathrm{d}\mathbf{F}}{\mathrm{d}z} = \mathbf{SF} \Leftrightarrow \left(\mathbf{S} - \mathbf{I}\frac{\mathrm{d}}{\mathrm{d}z}\right)\mathbf{F} = \mathbf{0}. \tag{4}$$

The general solution of this equation is

$$F_i = \sum_{\alpha=1}^{N} A_{i\alpha} C_\alpha \exp(\lambda_\alpha z), \qquad i \in [1, N] \tag{5}$$

where λ_α are the eigenvalues of the scattering matrix $\mathbf{S}$. $A_{i\alpha}$ is the matrix constructed with the eigenvectors corresponding to the eigenvalues λ_α. For a given $\mathbf{S}$ matrix, its eigenvalues appear in pairs (λ_a, λ_b), with $\lambda_b = -\lambda_a$. The spectrum of λ_α is related to different scattering lengths ${\lambda_\alpha}^{-1}$ of the eigenmodes

describing the scattering fluctuations in the medium [26]. Each eigenmode is described by the corresponding eigenvector associated with the eigenvalue λ_α, thus λ_α can be physically interpreted as the inverse of a penetration length of the associated eigenmode. The coefficients C_α are weighting coefficients that are determined using the boundary conditions at the interfaces.

2.2. *The scattering matrix*

Since we assume the medium to be isotropic, the intensity of scattered light depends only on the cosine of the scattering angle Ψ (figure 2), $\mathbf{u}_i.\mathbf{u}_j = \cos\Psi = \cos\theta_i\,\cos\theta_\mathrm{j} + \sin\theta_\mathrm{i}\,\sin\theta_\mathrm{j}\,\cos(\phi_\mathrm{i} - \phi_\mathrm{j})$. The amount of flux scattered into an element solid angle $\mathrm{d}\omega_i$ is then given by

$$\mathrm{d}^2F_i = -\frac{k_\mathrm{sca}F_j\mathrm{d}z}{\cos\theta_i}\frac{p(\mathbf{u_i}.\mathbf{u_j})\mathrm{d}\omega_i}{4\pi} \tag{6}$$

We now need to calculate the flux scattered from a beam travelling in a direction $\vec{\boldsymbol{u}}_i$ into channel i (defined by its angle θ_i, width $\mathrm{d}\theta_i$, and solid angle ω_i) in a solid angle delimited by ϕ_i and $\phi_i + \mathrm{d}\phi_i$ and equal to $\mathrm{d}\omega_i = \omega_i\mathrm{d}\phi_i/2\pi$ (figure 2). The total flux scattered into the ith channel is obtained by integrating over all azimuthal angles ϕ_i:

$$\mathrm{d}F_i = -\frac{k_\mathrm{sca}F_j\omega_i\mathrm{d}z}{8\pi^2\cos\theta_i}\int_0^{2\pi} p(\mathbf{u_i}.\mathbf{u_j})\mathrm{d}\phi_i \tag{7}$$

where

$$\int_0^{2\pi} p(\mathbf{u_i}.\mathbf{u_j})\mathrm{d}\phi_i = 2\pi\sum_{\ell=0}^{\nu_\mathrm{max}} a_\ell P_\ell(\cos\theta_i)P_\ell(\cos\theta_j) \equiv \tilde{\boldsymbol{p}}(\theta_i,\theta_j) \tag{8}$$

ν_max is the number of terms that have to be taken into account in the polynomial expansion whose evaluation will be discussed later in this section. Here a_ℓ are the projections of the phase function into the basis of orthogonal Legendre polynomials P_ℓ, that is,

$$a_\ell = \left(\ell + \frac{1}{2}\right)\int_{-1}^{1} p(u)P_\ell(u)\mathrm{d}u \tag{9}$$

Once the integration over ϕ_i is done, one can express elements s_ij as follows:

$$\begin{cases} \mathrm{s}_{ij} = \dfrac{k_\mathrm{sca}}{|\cos\theta_i|}\tilde{\boldsymbol{p}}(\theta_i,\theta_j)\omega_i, & i \neq j \\ \mathrm{s}_{jj} = -\dfrac{k_\mathrm{abs}}{|\cos\theta_j|} - \displaystyle\sum_{\substack{m=1 \\ m\neq j}}^{N}\mathrm{s}_{mj} = -\dfrac{k_\mathrm{ext}}{|\cos\theta_j|} \end{cases} \tag{10}$$

The first term of s_{jj} accounts for the contribution of absorption, while the second accounts for the decrease in channel j due to scattering into all other channels.

Off-axis illumination. When the illumination is off-axis, the symmetry around the z-axis is broken. In this case to solve equation (1) one must, as mentioned above, decouple the variables θ and ϕ by decomposing the flux F and the phase function p into Fourier series as,

$$F(\theta_j, \phi_j) = \sum_{m=0}^{\nu_{\max}} F^m(\theta_j) \cos(m\phi_j)$$

and

$$p(\mathbf{u_i}.\mathbf{u_j}) = \sum_{m=0}^{\nu_{\max}} (2 - \delta_{0m}) p^m(\theta_i, \theta_j) \cos[m(\phi_i - \phi_j)],$$

where $p^{\mathrm{m}}(\theta_i, \theta_j)$ is expanded into Legendre functions, that is,

$$p^m(\theta_i, \theta_j) = \sum_{\ell=m}^{\nu_{\max}} a_\ell \frac{(\ell - m)!}{(\ell + m)!} P_\ell^m(\cos\theta_i) P_\ell^m(\cos\theta_j).$$

Equation (1) becomes then a set of $\nu_{\max} + 1$ equations in which the unknowns are now the vectors $F^m(\theta_j)$, $j \in [1, N]$.

Scattering and absorption coefficients and the phase function: Mie theory. The phase function $p(\mathbf{u}_\mathrm{i}.\mathbf{u}_\mathrm{j})/4\pi$ represents the probability that radiation incident in the direction defined by (θ_j, ϕ_j), is scattered into the direction (θ_i, ϕ_i). If we now assume that the volume fraction of particles is small, so the independent-scattering approximation holds, the phase function will simply be the ratio between the differential scattering cross-section and the total scattering cross-section [27] of an isolated scatterer, that is

$$\frac{p(\mathbf{u_i}.\mathbf{u_j})}{4\pi} = \frac{1}{C_{\mathrm{sca}}} \frac{\partial C_{\mathrm{sca}}}{\partial \omega}(\mathbf{u_i}.\mathbf{u_j}). \tag{11}$$

In the case of spherical particles, the differential and total scattering cross-sections of an isolated sphere can be obtained from Mie theory [27]. Furthermore, since in the independent-scattering approximation the absorption, scattering and extinction coefficients k_{abs}, k_{sca} and k_{ext}, can be expressed in terms of the corresponding cross-sections C_{abs}, C_{sca} and C_{ext}, as $k_{\mathrm{abs}} = n_{\mathrm{p}} C_{\mathrm{abs}}$, $k_{\mathrm{sca}} = n_{\mathrm{p}} C_{\mathrm{sca}}$, $k_{\mathrm{ext}} = n_{\mathrm{p}} C_{\mathrm{ext}}$, one can also use Mie theory to determine them. Here n_{p} is the number of scatterers by unit volume. For the case of concentrated samples in which dependent scattering might play a role, one can calculate differential and total cross sections by using more sophisticated theories (see, for instance, [28, 29]). More generally, as the formulation of equation (1) depends only on the scattering parameters (k_{sca}, k_{ext}, $p(\mathbf{u}.\mathbf{u}')$), one can easily introduce adequate theories for the calculation of these terms with no harm to the generality of the method.

To compute the infinite polynomial expansion that appears in equation (8), one has to choose a finite number of terms ($\nu_{\max}$) to evaluate, which defines the accuracy of the evaluation of the phase function. The number of terms to be taken into account for an accurate numerical evaluation of the phase function is related to $n_{\max}$, the highest order chosen in the computation of the series expansion for the scattered field E_{sca}, as given by Mie theory, $p(\mathbf{u_i}.\mathbf{u_j}) \propto \left|E_{\mathrm{sca}}(\mathbf{u_i}.\mathbf{u_j})\right|^2$. Wiscombe's criterion [30] provides an accuracy lower than 10^{-14} for the calculation of E_{sca}, so taking $\nu_{\max} = 2 \times n_{\max}$ is generally sufficient.

3. Matrix formulation for the scattering medium

3.1. *The integration constants* C_α

The weighting coefficients C_α in equation (5) depend on the boundary conditions at the interfaces, and are usually determined at this step of the procedure [17–19], by introducing the reflectance and the transmittance factors of the interfaces. In order to totally decouple the behaviour of the scattering medium from its interfaces, we prefer to express this coefficients in terms of 'incident flux', that is the angular distribution of the scattering flux at $z = 0^+$ and at $z = Z^-$. Let $\mathbf{F^{inc}}$ denote the incident flux vector:

$$F_i^{\text{inc}} = F_i(0^+) \quad i \leq N/2, \qquad F_i^{\text{inc}} = F_i(Z^-) \quad i > N/2 \tag{12}$$

and A the matrix defined as follows:

$$\mathcal{A}_{i\alpha} = A_{i\alpha} \quad i \leq N/2, \qquad \mathcal{A}_{i\alpha} = A_{i\alpha} \exp(\lambda_\alpha Z) \quad i > N/2 \tag{13}$$

The coefficients C_α can then be expressed as

$$\alpha \in [1, N] \qquad C_\alpha = \sum_{i=1}^{N} a_{i\alpha} F_i^{\text{inc}}, \tag{14}$$

where $a_{i\alpha}$ are the elements of the inverse of matrix $\mathcal{A}$. In this way, the interfaces and the scattering media will be treated separately (see section 4).

3.2. *Flux evolution*

Expressions (13) and (14) allow us to directly express the flux vector at any arbitrary depth z as a function of the incident flux represented by a vector $\mathbf{F^{inc}}$:

$$\mathbf{F}(z) = \underbrace{\mathbf{G}(z)\mathcal{A}^{-1}}_{\mathbf{M}(z)} \mathbf{F^{inc}} \qquad \text{where } G_{i\alpha}(z) = A_{i\alpha} \exp(\lambda_\alpha z)$$

$$\mathbf{M}(z) = \begin{bmatrix} \mathbf{m}_a(z) & \mathbf{m}_b(z) \\ \mathbf{m}_c(z) & \mathbf{m}_d(z) \end{bmatrix} \tag{15}$$

$\mathbf{M}(z)$ is the matrix characterizing the evolution of the angular distribution of the flux along its propagation direction in the medium. The subindices a, b, c, and d split the matrix in blocks of size $N/2 \times N/2$ corresponding to the splitting of the channels in forward and backward directions. The matrix $\mathbf{M}(z)$ is the basis of our matrix representation. In figure 3 we illustrate the spatial evolution of the angular distribution of a light flux across a scattering medium with total thickness of 200 μm, filled with non-absorbing particles of size parameter 6.3 and a filling fraction of 0.1%. The host medium is air, the incidence beam is a plane wave traveling in the forward direction ($\theta = 0$) along $z > 0$, and we have taken $N = 50$ channels. From the bottom to the top, at increasing depth within the medium, one notices the isotropic distribution of the flux, i.e. an attenuation of the structures in the flux angular distribution. For example, at $z = 1$ μm there is a forward flux still concentrated mainly around $\theta = 0$, while the backward flux is more isotropic due to the backscattered process coming from most of the film ahead. At the middle of the film ($z = 100$ μm), the flux is more isotropic in both the forward a backward directions, while at the upper end, $z = 200$ μm, there is a rather isotropic distribution in the forward direction, and there is no flux in the backward direction because there is no material ahead that could provide a backscattering process.

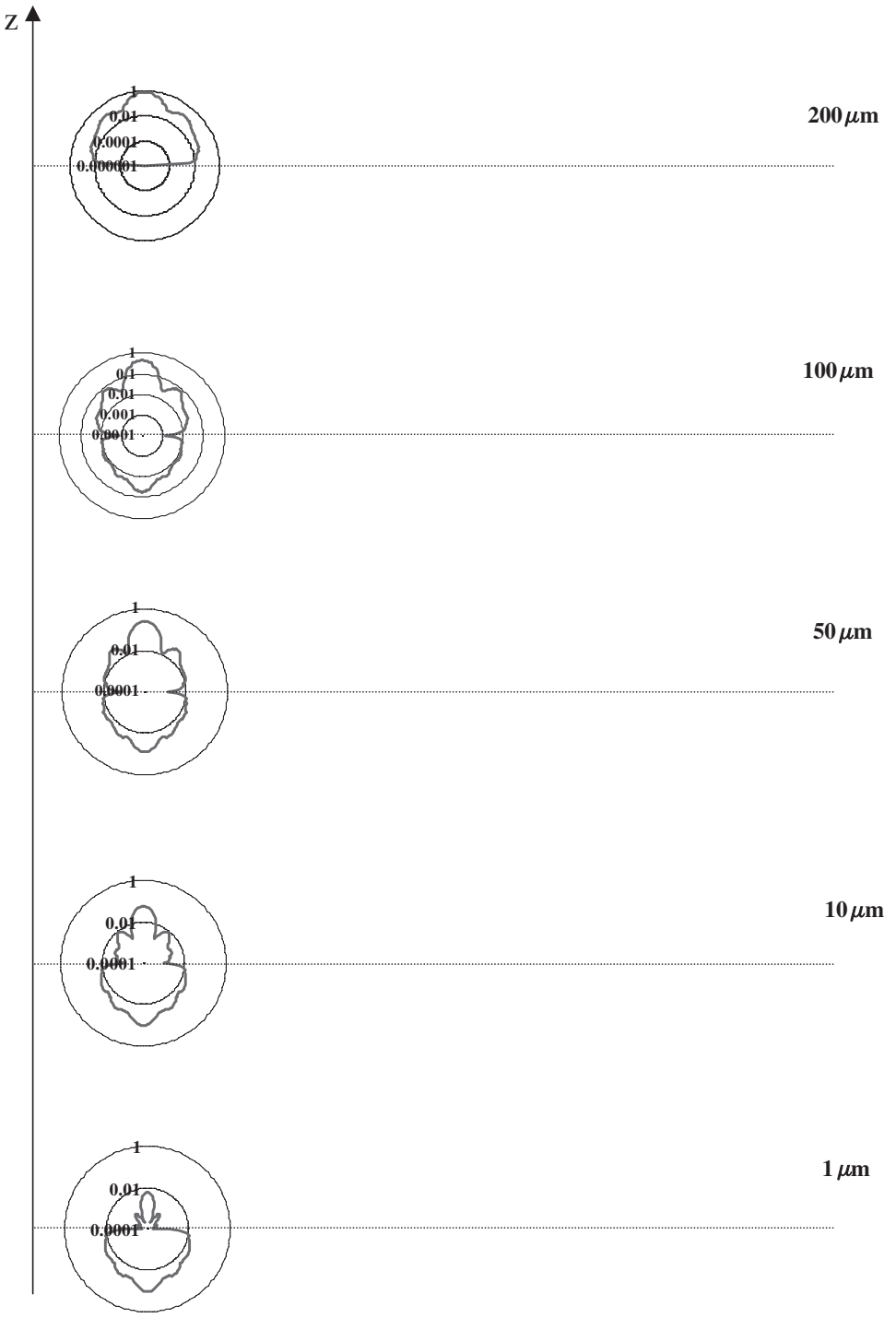

Figure 3. Example of evolution of the scattering profile for a non-absorbing scattering medium: size parameter 6.3, filling fraction 0.1%, thickness of medium 200 μm, host medium is air.

Overflows. One notices that in the expression for $\mathbf{M}(Z)$, $\mathcal{A}$ and $\mathbf{G}(Z)$ contain elements proportional to $\exp(\lambda_\alpha Z)$. These terms cause overflows when $\lambda_\alpha Z \geq 1$. Bearing in mind the pair behaviour of λ_α mentioned above, we propose the following solution to this problem. $\mathcal{A}$ can be expressed as the matrix product of α and δ defined as follows:

- if $\lambda_\alpha \geq 0$, $\quad \alpha_{i\alpha} = A_{i\alpha}\exp(-\lambda_\alpha Z)$ and $\delta_{\alpha\alpha} = \exp(\lambda_\alpha Z)$
- else, $\quad \alpha_{i\alpha} = A_{i\alpha}$ and $\delta_{\alpha\alpha} = 1$.

δ is diagonal and one can thus calculate $\mathcal{A}^{-1}$ as $\delta^{-1}\,\alpha^{-1} = \alpha^{-1}\,\delta^{-1}$, without any risk of overflow because α^{-1} and δ^{-1} only contain negative exponents. We follow the same process for $\mathbf{G}(z)$:

- if $\lambda_\alpha \geq 0$, $\quad \gamma_{i\alpha}(z) = A_{i\alpha}$ and $\delta_{\alpha\alpha}(z) = \exp(\lambda_\alpha z)$
- else, $\quad \gamma_{i\alpha}(z) = A_{i\alpha}\exp(\lambda_\alpha z)$ and $\delta_{\alpha\alpha}(z) = 1$.

One then can calculate $\mathbf{M}(z) = \gamma(z)\delta(z)\delta^{-1}\alpha$ where none of these matrices present numerical overflows except possibly δ. But there are no problems at $z = 0$ and $z = Z$ because $\mathbf{M}(0) = \mathbf{A}\alpha^{-1}$ and $\mathbf{M}(Z) = \gamma(z)\alpha^{-1}$. Therefore, at this step of the solution, the only matrix to be inverted is α.

4. The interfaces

We start by relating the outgoing flux from the slab of a scattering medium with total thickness Z, to the incident fluxes $F(0^+)$ and $F(Z^-)$. By outgoing flux we mean the flux that is about to leave the system just before the boundaries. The outgoing flux vector can be related to the incident fluxes via a matrix $\boldsymbol{\mathcal{M}}$, as

$$\mathbf{M} = \begin{bmatrix} \mathbf{m}_a(Z) & \mathbf{m}_b(Z) \\ \mathbf{m}_c(0) & \mathbf{m}_d(0) \end{bmatrix} \tag{16}$$

where $\boldsymbol{\mathcal{M}}(z)$ is the matrix derived in equation (15). Now we will take into account the role of the interfaces at $z = 0$ and $z = Z$, with figure 4 illustrating our synthetic notation. The reflectance and transmittance from medium i to medium j are denoted by R_{ij} and T_{ij}, respectively, the forward flux at $z = 0^+$ and $z = Z^-$ are denoted by F_a and F_b, respectively, while the backward flux by F_c and F_d. The outgoing flux vector is then written as $[F_b, F_c]^t$. First we define a new matrix, $\mathbf{P}$, derived from $\boldsymbol{\mathcal{M}}$, that relates the flux on the right-hand side of the slab to the ones on the left-hand side, and is given by,

$$\begin{bmatrix} F_b \\ F_\mathrm{d} \end{bmatrix} = \mathbf{P}\begin{bmatrix} F_a \\ F_c \end{bmatrix} \quad \text{where} \begin{cases} P_a = \mathcal{M}_a - \mathcal{M}_b\mathcal{M}_d^{-1}\mathcal{M}_c \\ P_b = \mathcal{M}_b\mathcal{M}_d^{-1} \\ P_c = -\mathcal{M}_d^{-1}\mathcal{M}_c \\ P_d = \mathcal{M}_d^{-1} \end{cases} \tag{17}$$

The conditions at the first interface, $z = 0$, can be written as follows:

$$\begin{cases} F_a = T_{12}F_{inc}(0) + R_{21}F_c \\ F_{out}(0) = T_{21}F_c + R_{12}F_{inc}(0) \end{cases} \tag{18}$$

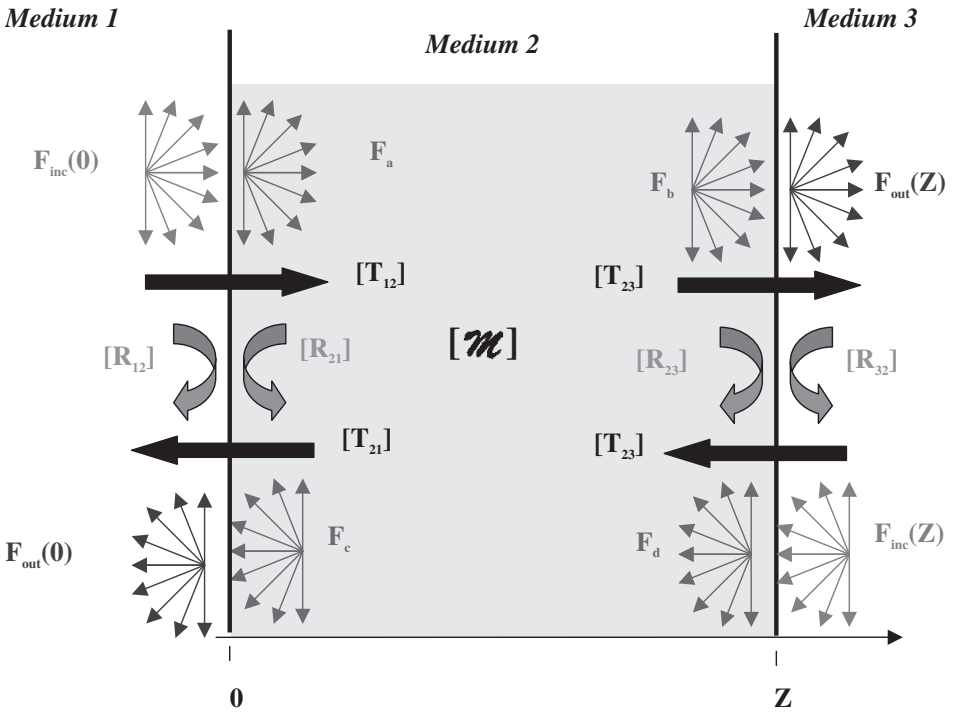

Figure 4. Simplified notation for matrix treatment.

where F_{out} denotes the flux that is leaving the system after crossing the boundaries. We can thus express the flux on the right-hand side of the first interface, as a function of the flux on the left-hand side, via a matrix β_{12},

$$\begin{bmatrix} F_a \\ F_c \end{bmatrix} = \begin{bmatrix} \beta_{12}(a) & \beta_{12}(b) \\ \beta_{12}(c) & \beta_{12}(d) \end{bmatrix} \begin{bmatrix} F_{\text{inc}}(0) \\ F_{\text{out}}(0) \end{bmatrix} \text{ where } \begin{cases} \beta_{12}(a) = T_{12} - R_{21} T_{21}^{-1} R_{12} \\ \beta_{12}(b) = R_{21} T_{21}^{-1} \\ \beta_{12}(c) = -T_{21}^{-1} R_{12} \\ \beta_{12}(\text{d}) = T_{21}^{-1} \end{cases} \tag{19}$$

In the same way, we can define β_{23} at the second interface, as

$$\begin{bmatrix} F_{\text{out}}(Z) \\ F_{\text{inc}}(Z) \end{bmatrix} = \begin{bmatrix} \beta_{23}(a) & \beta_{23}(b) \\ \beta_{23}(c) & \beta_{23}(d) \end{bmatrix} \begin{bmatrix} F_b \\ F_d \end{bmatrix} \text{ where } \begin{cases} \beta_{23}(a) = T_{23} - R_{32} T_{32}^{-1} R_{23} \\ \beta_{23}(b) = R_{32} T_{32}^{-1} \\ \beta_{23}(c) = -T_{32}^{-1} R_{23} \\ \beta_{23}(d) = T_{32}^{-1} \end{cases} \tag{20}$$

Combining equations (19) and (20), we can write:

$$\begin{bmatrix} F_{\text{out}}(Z) \\ F_{\text{inc}}(Z) \end{bmatrix} = \boldsymbol{\beta_{23}} \overbrace{\mathbf{P}\boldsymbol{\beta_{12}}}^{\mathbf{Q}} \begin{bmatrix} F_{\text{inc}}(0) \\ F_{\text{out}}(0) \end{bmatrix} \tag{21}$$

We thus have a simple expression for the angular distribution of the flux at one side of the slab as a function of the angular distribution of the flux at the other side.

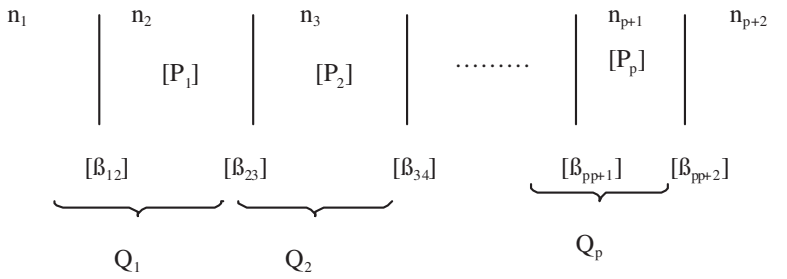

Figure 5. Multilayer representation.

This expression is easily generalized to a multilayer composed of p slabs (see figure 5), as

$$\begin{bmatrix} F_{\text{out}}(Z_{\text{tot}}) \\ F_{\text{inc}}(Z_{\text{tot}}) \end{bmatrix} = \boldsymbol{\beta}_{\mathbf{p+1,\,p+2}} \underbrace{\mathbf{Q_p Q_{p-1}} \cdots \mathbf{Q_2 Q_1}}_{\mathbf{Q_{p-slabs}}} \begin{bmatrix} F_{\text{inc}}(0) \\ F_{\text{out}}(0) \end{bmatrix} \tag{22}$$

This expression is formally similar to the one used in the treatment light transport in non-scattering multilayers [20]. Reflectance matrices $\mathbf{R_{pq}}$ are anti-diagonal: a flux incident in channel i will be reflected into channel $N-i$. The structure of transmittance matrices $\mathbf{T_{pq}}$ is more complicated due to the possible occurrence of a critical angle θ_q^{crit} ($n_q \sin\theta_q^{\text{crit}} = n_p$, if $n_q > n_p$) above which the transmittance is zero and the reflectance is one. Such ill-conditioned matrices are difficult to invert. To avoid this problem, another space discretization has to be defined. We regard the refraction cone as the region where flux can emerge from the slab, and discretize it into N channels. Another space discretization (N' channels) is made for solid angles not belonging to the refraction cone. In that region, we take into account the possibility that a quantity of flux scattered in that zone will be scattered into the refraction cone. The problem when dealing with the multilayered problem is that the dimensions of the matrices must be properly defined. Indeed, as the spatial discretization in each layer is different, we have to deal with rectangular matrices.

5. Results

First, we compare our predictions on two scattering slabs with very different scattering behaviours (Rayleigh and Mie scattering), with those obtained using a Monte Carlo method [21] and using the 4-flux theory [22]. Then, we couple these two media and calculate, using the matrix procedure described above, the optical properties of this bi-slab under normal incidence and $\lambda = 0.55\,\mu\text{m}$. Finally, as another example of the worth of the proposed matrix procedure, we calculate the optical properties of a system composed of five layers: two scattering media (latex beads suspensions) bounded by silica plates, under normal incidence and $\lambda = 0.589\,\mu\text{m}$.

5.1. *Slabs with very different scattering behaviour*

The input parameters that characterize each medium are given in table 1. Medium 1, with spherical scatterers of size parameter 0.76, has a relatively isotropic phase function (figure 6). In contrast, the phase function of medium 2, with spherical scatterers of size parameter 17.1, presents a strong anisotropy, with

Table 1. Input parameters for medium 1 and 2 and scattering parameters calculated by Mie theory

	Medium 1	Medium 2
Spheres radius (μm)	0.05	1.0
Index of refraction of the spheres	$1.5+\mathrm{i}\ 10^{-4}$	$2.7+\mathrm{i}\ 10^{-4}$
Size parameter *ka*	0.76	17.1
Scatterers volume fraction (%)	1	0.1
Scattering coefficient k_{sca} (μm^{-1})	7.57×10^{-4}	1.62×10^{-3}
Extinction coefficient k_{ext} (μm^{-1})	7.80×10^{-4}	1.63×10^{-3}
Medium thickness (μm)	1000	1000
Index of refraction of the host medium	1.333	1.5

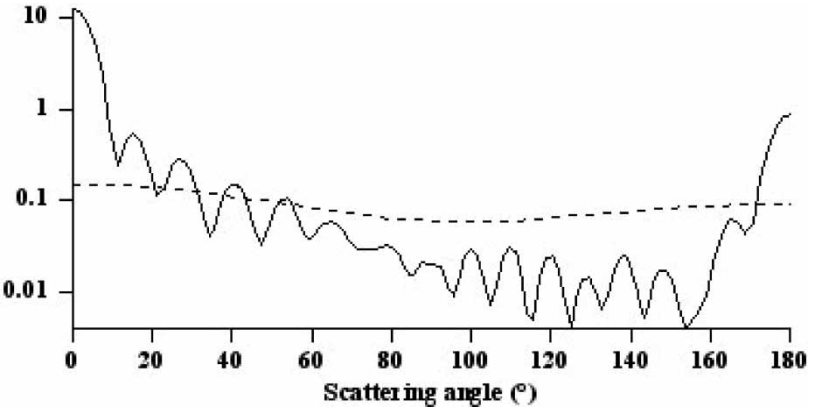

Figure 6. Phase functions for medium 1 (- - - -) and medium 2 (——).

predominant scattering in the forward direction and the presence of scattering lobes.

The discretization of the phase function depends on its structure. A phase function with a lot of structure requires a finer discretization, in order to preserve the relevant information in the phase function structure. The number N of channels must be larger than the number of Legendre polynomials ν_{max} (equation (8)) required in the expansion of the phase function, in our case we have $\nu_{max} = 10$ for medium 1 and $\nu_{max} = 44$ for medium 2. Here we have chosen a space discretization with $N = 20$ for medium 1 and with $N = 100$ for medium 2. The scattering and extinction coefficients calculated by Mie theory are given in table 1. In table 2, we display a comparison between the optical properties (collimated and total reflectance and transmittance coefficients) obtained by the proposed method and the results obtained using the Monte Carlo method and using 4-flux theory.

Monte Carlo calculation. The Monte Carlo method provides a statistical evaluation of integrals for quantities obeying statistical laws. The multiple scattering process of light within a scattering medium can also be regarded as the flux of particles, conventionally called 'photons', each of them with a certain probability to disappear between depth z and depth $z+\mathrm{d}z$. The probability $\mathrm{d}P$ for a photon to disappear in $\mathrm{d}z$ because of absorption and scattering processes is defined as

Table 2. Collimated transmittance (Tc) and reflectance (Rc); Scattered transmittance (Ts) and reflectance (Rs), Absorption (A) obtained with Monte Carlo, 4-flux and N-flux models

			T_c	R_c	T_s	R_s	A
Monte Carlo	Medium 1	Values	0.4406	0.0244	0.2567	0.2122	0.0661
		$\pm$[1]	–	–	2.0×10^{-3}	2.2×10^{-3}	3.9×10^{-3}
	Medium 2	Values	0.181	0.0415	0.5238	0.2336	0.0201
		$\pm$[1]	–	–	1.4×10^{-3}	2.1×10^{-3}	7.1×10^{-3}
4-flux	Medium 1	$\varepsilon = 1.488$[(2)]	0.4401	0.0245	0.2474	0.2297	0.0674
	Medium 2	$\varepsilon = 1.282$[(2)]	0.1811	0.0415	0.5334	0.2345	0.0098
N-flux	Medium 1	20 channels	0.4401	0.0245	0.256	0.2169	0.0625
	Medium 2	100 channels	0.1811	0.0414	0.5237	0.2338	0.0201
∂(NF-MC) [(3)]	Medium 1	–	–	–	-7×10^{-4}	5×10^{-3}	-4×10^{-3}
	Medium 2	–	–	–	-1×10^{-4}	-2×10^{-4}	3×10^{-5}

[1]Accuracy.
[2]Assymetry parameter in 4-flux theory.
[3]Difference between values given by N-flux (NF) and Monte Carlo (MC) calculation.

$dP = k_{abs}dz$ and $dP = k_{sca}dz$, respectively, while the probability that a photon will be scattered in the direction $\mathbf{u}'$ with a solid angle $d\omega'$ is given by $P(\mathbf{u}.\mathbf{u}')d\omega'/4\pi$. A balance of the energy flux made on the number of particles per unit volume leads to the RTE, written for the number of 'photons' per unit volume. Under these circumstances there is a full equivalence between these particles and flux, and the integral in the RTE can be statistically evaluated by the Monte Carlo method.

The disadvantage of this method is that the results present statistical fluctuations and the accuracy of the final results (reflection, transmission and absorption) is only proportional to $\mathcal{N}^{-1/2}$, where $\mathcal{N}$ is the number of particles. To get rid of this problem, one has to work with a large number of particles, leading to calculation times that can sometimes be extremely long. The results obtained by a Monte Carlo calculation presented in table 2, have been computed for $\mathcal{N} = 10^6$, providing an accuracy of the order of 10^{-3}. The difference between the Monte Carlo simulations and our results are between 10^{-5} and 2×10^{-3}. Thus we conclude that the proposed model provides results with very much the same accuracy as those obtained using the Monte Carlo method. We present the angular distribution of the scattering flux as a function of the scattering angle in figure 7(a) and (b); angles between 0° and 90° correspond to the transmitted flux. We can see

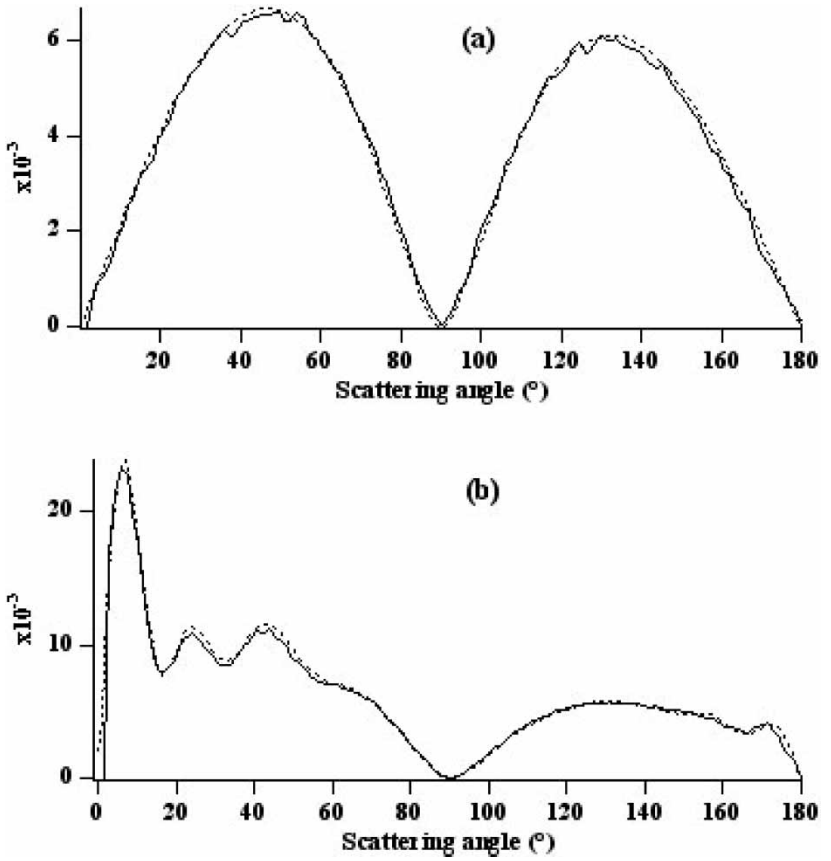

Figure 7. Comparison between N-flux method (- - - - -) and Monte Carlo method (——): angular distribution of fluxes for medium 1 (a) and medium 2 (b).

that the angular distribution obtained with our procedure is also very close to the one obtained using the Monte Carlo method. As mentioned above, the Monte Carlo method is very time consuming. We performed N-flux and Monte Carlo computations with a Macintosh G4 computer (256 Mb RAM, 400 MHz): for medium 1, the N-flux method required 0.82 s and the Monte Carlo method required 62 s; for medium 2, 42 s for N-flux and 87 s for Monte Carlo.

4-flux calculation. The 4-flux theory is a simplified method for solving the RTE. The quantities considered in this theory are the collimated reflected and transmitted fluxes, obeying the Beer–Lambert law, and the forward and backward scattered fluxes, integrated over all directions in each hemisphere. After this integration is performed, the equations still depend on an asymmetry coefficient ε, which depends on the angular distribution of scattered quantities, and is given by, $\varepsilon = \int_0^1 F(z,\theta)\mathrm{d}(\cos\theta)/\int_0^1 F(z,\theta)\cos\theta\mathrm{d}(\cos\theta)$. With this method, it is not possible to determine ε because this requires $F(z,\theta)$ whose calculation is beyond the scope of the method itself. Usually ε has to be chosen arbitrarily, between 2, for an isotropic distribution of scattered flux, and 1 for a very anisotropic angular distribution. Nevertheless, taking into account our previous calculations of $F(z,\theta)$, we determined values of ε of 1.488 for medium 1 and 1.282 for medium 2.

The results given by the 4-flux method are less accurate than ours: we can estimate an accuracy of the order of 10^{-2} for 4-flux, while it was 10^{-3} for the N-flux method when compared with the Monte Carlo calculation. This lack of accuracy can be attributed to the fact that scattering properties are taken into account only in an average way:

(i) locally, the asymmetry of the phase function is taken into account via the so-called asymmetry parameter g (integration of the phase function weighted by $\cos\theta$)
(ii) at the macroscopic scale, the asymmetry of the flux angular distribution is taken into account via the asymmetry coefficient ε.

In both cases, this leads to an overestimation of the total scattered flux.

5.2. *A two-layered slab*

We now present an example that illustrates the use of the multislab model. Here we construct a bi-slab composed of the two scattering layers described above. Figure 8 displays the angular distribution of the scattered flux by unit solid angle for each layer. The backward direction (reflectance) corresponds to angles belonging to interval $[\pi/2,-\pi/2]$. When these two layers are put together, one notices (figure 9) that the presence of medium 1 (Rayleigh scattering behaviour) modifies the shape of the scattering profile (full curve) very little. The thickness of medium 2 (Mie scattering behaviour) has to be reduced by a factor of 100 (dashed curve) to attenuate the dominant Mie behaviour enough to enter the Rayleigh regime.

5.3. *A multislab composed of five layers*

In this section we present an example of a calculation more related to experiments of practical interest. A sketch of the system is shown in figure 10: it is composed of a Rayleigh-type suspension of latex beads (medium 2) between two silica plates (medium 1 and 3) put together with a Mie-type suspension of latex beads (medium 4) between two silica plates (medium 3 and 5). The input

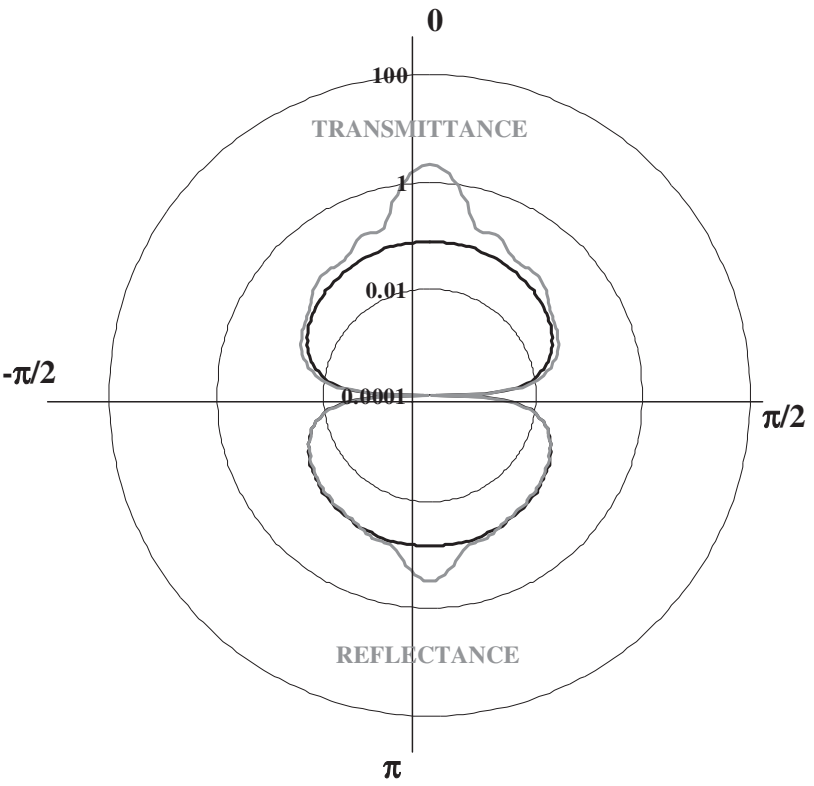

Figure 8. Fluxes by unit solid angle for medium 1 (——) and medium 2 (——).

parameters for each layer are summarized in table 3. The phase functions of the two scattering media are shown in figure 10. Due to the different number of structures showing up in the phase function of medium 4 ($\nu_{max} = 53$), the discretization number N is taken equal to 120.

In figure 11 we present results for the optical properties of this system: the transmittance clearly exhibits a Mie type behaviour (more appreciable in linear scale) while the reflectance behaves like the first medium crossed by the incident light, i.e. Rayleigh dominant. Because of the strong scattering anisotropy of medium 4 and of its thickness, which is ten times weaker than that of medium 2, the detection of the Mie type medium is essentially visible in transmittance, and the backscattering effects produced by medium 4 are destroyed in the propagation through medium 2.

6. Conclusions

In this paper we have developed a matrix procedure for solving the problem of light scattering by multilayered media. By separating the volume-scattering behaviour from the properties of interfaces, we have achieved a complete matrix solution with the same structure as the one already known for the case of non-scattering media. We have used the Discrete Ordinate Method to solve the Radiative Transfer Equation (N-flux), and we have compared the results obtained for a single slab with other methods (Monte Carlo and 4-flux calculations),

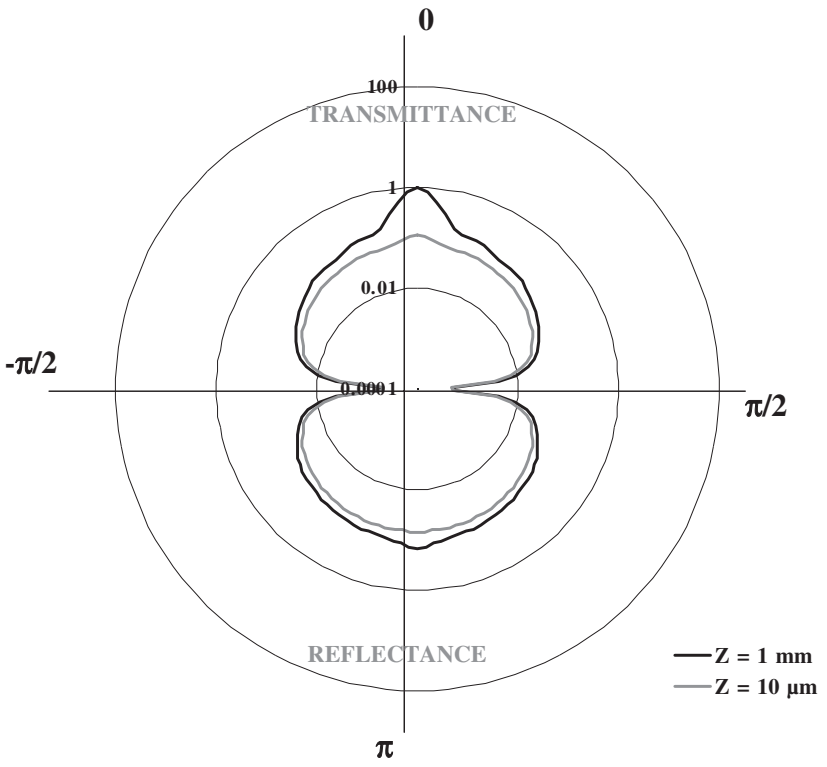

Figure 9. Fluxes by unit solid angle: medium 1 and 2 coupled.

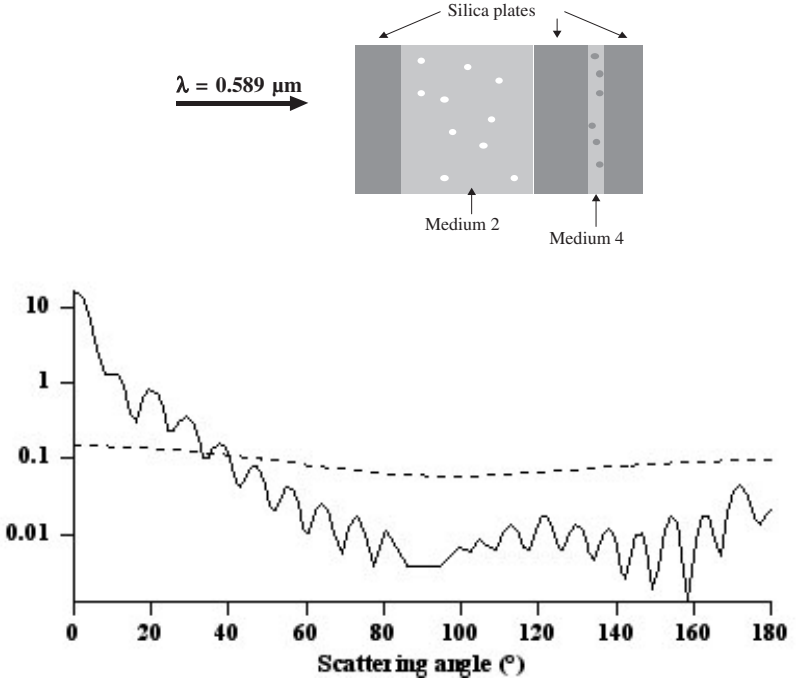

Figure 10. Phase functions for medium 2 (- - - -) and medium 4 (——).

Table 3. Input parameters for the multilayered slab

	Medium 1	Medium 2	Medium 3	Medium 4	Medium 5
Spheres radius (μm)	–	0.05	–	1.5	–
Spheres index	–	1.5905	–	1.5905	–
Medium thickness (μm)	1500	1000	2700	100	1100
Medium index	1.458	1.333	1.458	1.333	1.458
Scatterers volume fraction (%)	–	1.5	–	4.0	–

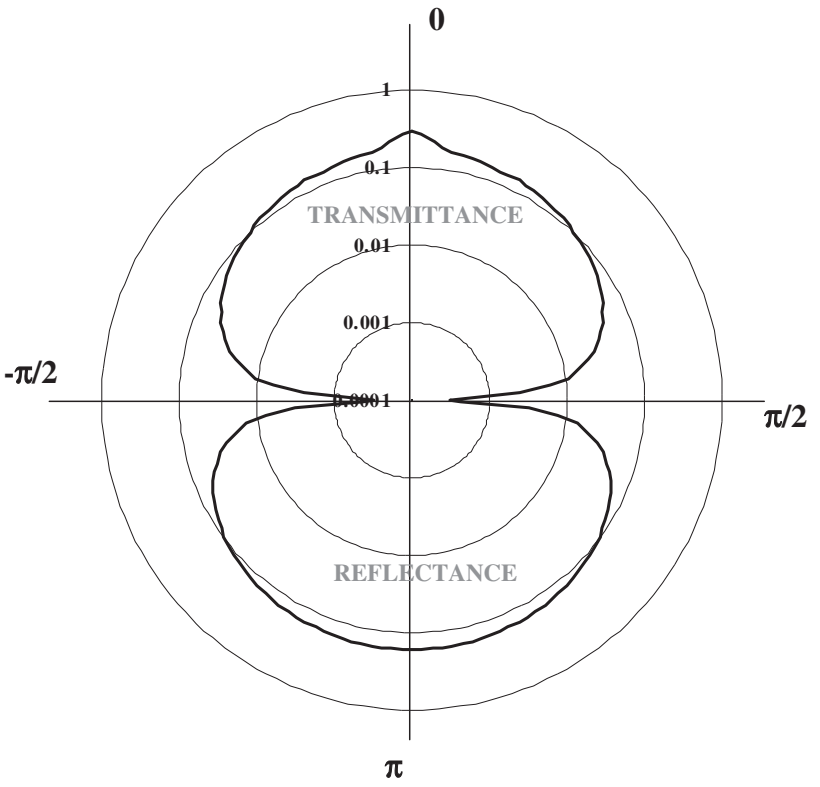

Figure 11. Fluxes by unit solid angle for the multislab.

yielding a proof of the accuracy of the *N*-flux method. We then built a matrix procedure to extend the *N*-Flux method to a multislab system by introducing suitable scattering laws for volume and interfaces. A comparison with another semi-analytical method [31] has been handled and is to be published. This simplified formulation allows the separate treatment of the volume and the interfaces. This separation becomes very convenient when one wants to extend the treatment to non-spherical particles (volume) or to include the roughness of the interfaces. Even if there are few matrix inversions, this method is very fast in so far as the dimensions of the matrices generated are related to the particles size parameter and in general do not need to be very large. Consequently this method can be introduced in a fit algorithm to recover, by comparison with optical measurements, geometric characteristics of the scattering medium (number of

slabs, thickness of each slab) and the nature of its constituents (relative index of refraction and shape of the scatterers, size parameter, volume fraction). This method can be used for a large set of fundamental (modelling of atmospheres, interstellar particles), industrial applications (paints, papers, cosmetics), and also biomedical diagnosis (modelling of light scattered by human skin).

References

[1] Chandrasekar, S., 1960, *Radiative Transfer* (New York: Dover Publications).
[2] Kourganov, V., 1963, *Basic Methods in Transfer Problems* (Oxford: Oxford University Press).
[3] Lagendiijk, A., and van Tiggelen, B. A., 1996, *Phys. Rep.*, **270,** 2145.
[4] Yodh, A., and Chance, B., 1995, *Phys. Today*, **48**(3)**,** 34.
[5] Tsang, L., 1985, *Theory of Microwave Remote Sensing,* Wiley series in remote sensing (New York: John Wiley & Sons).
[6] Kuga, Y., Ulaby, F. T., Haddock, T. F., and DeRoo, R., 1991, *Radio Sci.*, **26,** 329.
[7] Fung, A. K., 1994, *Microwave Scattering and Emission in Random Media* (Artech House).
[8] Schuster, A., 1905, *Astrophys. J.*, **12,** 12.
[9] Schwarzschild, K., 1906, *Ges. Wiss. Gottingen. Nachr., Math-Phys. Klasse*, **1,** 41.
[10] Schwarzschild, K., 1914, *K. Berl. Ber. Math. Phys. Kl.*, 1183.
[11] Wick, G. C., 1943, *Z. Phys.*, **120**.
[12] Lathrop, K. D., and Carlson, B. G., 1965, Los Alamos Scientific Laboratory Report, 3186.
[13] Fiveland, W. A., 1987, *Trans. ASME, J. Heat Transfer*, **109,** 809.
[14] Mudgett, P., and Richards, L. W., 1971, *Appl. Opt.*, **10,** 1485.
[15] Stamnes, K., and Swanson, R., 1981, *J. Atmos. Sci.*, **38,** 387.
[16] Jin, Zh., and Stamnes, K., 1994, *Appl. Opt.*, **33,** 431.
[17] Stamnes, K., and Conklin, P., 1984, *J. Quant. Spectrosc. Radiat. Transfer*, **31,** 273.
[18] Stamnes, K., 1986, *Rev. Geophys.*, **24,** 299.
[19] Liou, B.-T., and Wu, C.-Y., 1996, *Heat Mass Transfer*, **32,** 103.
[20] Abelès, F., 1950, *Ann. Phys.* (Paris), **5,** 706.
[21] Briton, J.-P., Maheu, B., Grehan, G., and Gouesbet, G., 1992, *Particle Particle Syst. Characterization*, **9,** 52.
[22] Beasley, J. K., Atkins, J. T., and Billmeyer Jr., F. W., 1967, *Electromag. Scattering*, 765.
[23] Vasalos, I. A., 1970, *J. Heat Transfer*, **92,** 285.
[24] Schulz, F. M., Stamnes, K., and Weng, F., 1999, *J. Quant. Spectrosc. Radiat. Transfer*, **61**(1)**,** 105.
[25] Kim, A. D., and Ishimaru, A., 1999, *J. Computat. Phys.*, **152,** 264.
[26] Bohren, C. F., and Huffman, D. R., 1983, *Absorption and Scattering of Light by Small Particles* (New York: Wiley-Interscience).
[27] Mie, G., 1908, *Ann. Phys.*, **25,** 377.
[28] Stout, D. B., Auger, J.-C., and Lafait, J., 2001, *J. Mod. Opt.*, **109,** 2105.
[29] da Silva, A., Andraud, C., Charron, E., Stout, B., and Lafait, J., Multiple light scattering in multilayered media: theory, experiments'', Physica B (to be published).
[30] Wiscombe, W., 1980, *J. Appl. Opt.*, **19,** 1505.
[31] Elias, M., and Elias, G., 2002, *J. Opt. Soc. Am. A*, **19,** 894.